J. Am. Chem. Soc. **1986**, *108*, 196-206

A Theoretical Study of Successive Hydrogenations of Small Platinum Clusters: Structure and Energetics

Christian Minot,*[†,1] Bernard Bigot,*[‡,1] and Atika Hariti[‡]

Contribution from the Laboratoire de Chimie Théorique, Université de Paris Sud, 91405 Orsay Cedex, France, Laboratoire de Chimie Organique Théorique, Université Pierre et Marie Curie, 4 place Jussieu 75230 Paris, France, and Ecole Normale Supérieure de Saint-Cloud, 92211 Saint-Cloud, France. *Received December 26, 1984*

Abstract: The successive hydrogenations, up to saturation, of the most stable small platinum clusters Pt_n (n = 2–13) are studied by the extended Hückel method with (EHT-SO) and without (EHT) spin–orbit coupling. For each hydrogenation step, a large number of possible structures has been calculated in order to determine the stereochemistry of the best stepwise hydrogenated compounds. The results indicate that the energies of the first successive steps of dihydrogen adsorptions on the small clusters decrease stepwise with the hydrogenation rate, except for a few steps which are discussed. In these conditions, if the hydrogenation reactions are either under thermodynamic control or under kinetic control with activation energies related to the reaction enthalpies, all the clusters of a given size will adsorb a first H_2 molecule before one of them can adsorb a second molecule. Another remarkable point is that the energy of first adsorption varies with the cluster size. It shows a peak for Pt_3 and Pt_4 that makes the Pt_3 and Pt_4 species the most likely clusters to be hydrogenated first in a collection of clusters of different size. Thus, the successive plateaux of hydrogenation recently observed by Fraissard on platinum clusters supported on zeolites might be interpreted as a quantitative determination of the number of the Pt_3 and Pt_4 clusters in a catalytic system. The structure of the best hydrogenated clusters can be viewed as the progressive buildup of a three-dimensional network of square-planar and/or octahedral platinum complexes sharing hydrogen ligands along one common vertex or edge. These local geometries are associated with formal $Pt^{II}(d^8)$ and $Pt^{IV}(d^6)$ oxidation states, resulting from one or two oxidative additions ($H_2 \rightarrow 2H$) per platinum and an appropriate number of molecular adsorptions. For comparison, hydrogenation of the (111) face of platinum cyrstal has been studied for different coverages. Similar features are observed for both clusters and surfaces.

I. Introduction and Scope.

Transition-metal clusters are nowadays the subject of a large number of both experimental[2] and theoretical[3,4] studies. Part of this interest is related to their structural diversity and to their potentiality to give insight into the origin of the catalytic properties of metallic species by serving as bridges between molecular and solid-state chemistry. Hydrogenation reactions occupy a central place in fundamental research[5] as well as in industrial processes. Recently Fraissard et al.[6] detected unusually small platinum clusters supported on zeolites (the estimated average number of atoms per cluster is eight) and studied their first hydrogenation steps. So far, experiment does not yield the detailed structure and energetics of the hydrogenated specie. Despite a lot of experiments, hydrogen on a platinum surface is not a system completely understood either. The present calculations on the compounds involved in the stepwise progression from the naked aggregates (or surface) to the fully hydrogenated structures provide useful complementary information on these topics.

In a preceding paper,[3] a systematic study of the stability of the naked Pt_n clusters (n = 2, 13 atoms) has been carried out at the EHT level with and without spin–orbit coupling. The present study concerns the hydrogenation of the most stable clusters and assumes that there is no relaxation of the metallic framework during the successive hydrogenation steps. Calculations on numerous Pt_nH_{2p} structures have been carried out in order to determine the most stable isomers; here p is the number of adsorbed dihydrogen molecules; it varies from 1 to a maximum value p_{max}; p_{max} corresponds to saturation and is defined as the value for which any supplementary adsorption ($Pt_nH_{2p_{max}} + H_2 \rightarrow Pt_nH_{2(p_{max}+1)}$) is energetically unfavorable, whatever the organization of the $2p_{max} + 2$ hydrogen atoms on the clusters is.

This report focuses on the properties of the first hydrogenation steps to understand the recent observations provided by nuclear magnetic resonance (NMR) experiments and on the saturated hydrogenated species because of their analogy with other molecular clusters. Furthermore, these results are compared to those obtained for some hydrogenation modes upon (111) Pt surfaces.

The present study concerns the energetics and the structure of the various intermediates occurring in the successive steps of

---

[†] Université de Paris Sud.

[‡] Université Pierre et Marie Curie.

(1) These laboratories are part of U. A. 506 of CNRS.

(2) Johnson, B. F. G. "Transition Metal Clusters": Wiley-Interscience: Chichester, England, 1980. Mingos, D. M. P. "Comprehensive Organometallic Chemistry"; Stone, Wilkinson, Eds.; Pergamon Press: Oxford, 1982. Chini, P. *Gazz. Chim. Ital.* **1979**, *109*, 225. F. Cyrot-Lackmann, F., Ed. "Entre l' atome et le cristal:les agrēgats"; 4ème Ecole d'ētē Mēditerranēenne, Aix-en-Provence, Les ēditions de Physique, 1981. Bruce, M. I. *J. Organomet. Chem.* **1983**, *242*, 147, 417. Muetterties, E.; Rhodin, T. N.; Band, E.; Brücker, C. F.; Pretzer, W. R. *Chem. Eng. News* **1982**, *August 30*, 28–40. Muetterties, E. *Chem. Rev.* **1979**, *79*, 91. Gallezot, P. *Surf. Sci.* **1981**, *106*, 459. Gallezot, P. *J. Chim. Phys.* **1981**, *78*, 881. Gallezot, P.; Bienenstock, A.; Boudart, M. *Nouv. J. Chim.* **1978**, *2*, 263. See also references in ref 3.

(3) Bigot, B.; Minot, C. *J. Am. Chem. Soc.* **1984**, *106*, 6601.

(4) Teo, B. K. *Inorg. Chem.* **1984**, *23*, 1251. Evans, D. G. *J. Chem. Soc., Chem. Commun.* **1983**, 675. Mingos, D. M. P. *Nature* (*London*), *Phys. Sci.* **1972**, *236*, 99. Wade, K. *Chem. Br.* **1975**, *11*, 177. Wade, K. *Adv. Inorg. Chem. Radiochem.* **1976**, *18*, 1. Wade, K. *Chem. Commun.* **1971**, 792. Robertson, J. C.; Wilmensen, C. W. *J. Vac. Sci. Technol.* **1972**, *9*, 901. Minot, C.; Criado-Sancho, M. *Nouv. J. Chim.* **1984**, *537*, 8. See also ref 3 and references therein.

(5) For theoretical studies, see: Weinberg, W. H.; Merrill, R. P. *Surf. Sci.* **1972**, *33*, 493. Baetzold, R. C. *Surf. Sci.* **1975**, *51*, 1. Baetzold, R. C. *J. Am. Chem. Soc.* **1983**, *105*, 4271. Shusterovich, E. *J. Phys. Chem.* **1983**, *87*, 14. Shusterovich, E. *J. Am. Chem. Soc.* **1980**, *102*, 5989. Shusterovich, E. *J. Phys. Chem.* **1982**, *86*, 3114. Shusterovich, E. *Solid State Commun.* **1982**, *44*, 567. Blomberg, M. R. A.; Siegbahn, P. E. *J. Chem. Phys.* **1983**, *78*, 5682. Upton, T. H.; Goddard, W. A. *Phys. Rev. Lett.* **1979**; *42*, 472. Muscat, J. P.; Newns, D. M. *Surf. Sci.* **1980**, *99*, 609. Melius, C. F.; Moskowitz, J. W.; Mortola, A. P.; Baillie, M. B.; Ratner, M. A. *Surf. Sci.* **1976**, *59*, 279. Basch, H.; Newton, M. D.; Moskowitz, J. W. *J. Chem. Phys.* **1980**, *73*, 4492. Louie, S. *Phys. Rev. Lett.* **1979**, *42*, 476. Messmer, R. P.; Salahub, D. R.; Johnson, K. H.; Yang, C. Y. *Chem. Phys. Lett.* **1977**, 5184. Saillard, J.-Y.; Hoffmann, R. *J. Am. Chem. Soc.* **1984**, *106*, 2006. Gavezzotti, A.; Tantardini, G. F.; Simonetta, M. *Chem. Phys.* **1984**, *84*, 453. Ellis, D. E.; Adachi, H.; Averill, F. W. *Surf. Sci.* **1976**, 497. Van der Avoird, A.; de Graaf, H.; Bern, R. *Chem. Phys. Lett.* **1977**, *48*, 407. Kobayashi, H.; Yoshida, S.; Kato, H.; Fukui, K.; Tarama, K. *Surf. Sci.* **1979**, *79*, 189. Sevin, A.; Chaquin, P. *Nouv. J. Chim.* **1983**, *7*, 353. Sevin, A. *Nouv. J. Chim.* **1981**, *5*, 233. Dunken, H.; Jemmis, E. D. *Z. Chem.* **1983**, *20*, 454. For experimental studies, see: Christmann, K.; Ertl, G.; Pignet, T. *Surf. Sci.* **1976**, *54*, 365. Chistmann, K.; Behm, R. G.; Ertl, G.; Van Hove, M.; Weinberg, W. H. *J. Chem. Phys.* **1979**, *70*, 4168. Baro, A. M.; Ibach, H.; Bruchmann, H. D. *Surf. Sci.* **1979**, *88*, 384. Lapoulajade, J.; Neil, K. S. *J. Chem. Phys.* **1973**, *70*, 798. Norton, P. R.; Davies, J. A.; Jackman, T. E. *Surf. Sci.* **1974**, *65*, 189. Lu, K. E.; Rye, R. R. *Surf. Sci.* **1974**, *45*, 677. Salmeron, M.; Gale, R. J.; Somorjai, G. A. *J. Chem. Phys.* **1979**, *70*, 2807.

0002-7863/86/1508-0196$01.50/0

Table I. Parameters Used in EHT Calculations

orbital	H_{ii} (eV)	$\exp_1$	$\exp_2$	c_1	c_2
5d Pt	−12.59	6.013	2.696	0.6334	0.5512
6s Pt	−10.00	2.554			
6p Pt	−5.475	2.554			
1s H	−13.60	1.300			

hydrogenation; the details of the reaction paths are not analyzed and thus the conclusions presently drawn are exclusively relevant if we assume that the hydrogenation steps are either under thermodynamic control or under kinetic control with activation energies parallel to the enthalpies (Hammond postulate).

II. Calculation Methods

In the present paper, two types of calculations are presented. They are extended Hückel[7] calculations on the hydrogenated platinum clusters and band calculations on various hydrogenation modes of a platinum *fcc* surface. In the former case, the method used is a crystalline extension[8] of the EHT program within the tight-binding scheme. The same parameters are used for both types of calculations; they are listed in Table I. The off-diagonal hamiltonian matrix elements are derived from the diagonal terms on using the weighted H_{ij} formula.[9a] Those parameters have been previously used in ref 3 and 8b. They provide a reasonable dispersion band for the platinum crystal. No charge iteration procedures[9b] have been performed despite the large net charges calculated on the hydrogenated platinum clusters (from 0.5 to 2.2 e). The SO coupling terms are introduced in the matrix elements concerning spin-orbitals as in ref 3. The parameter ξ of the platinum atom is 0.62451 eV.

Throughout this study, platinum–platinum and platinum–hydrogen bond lengths are maintained at constant values of 2.77 and 1.6 Å, respectively. The metal–metal value was already used in previous studies; it is in agreement with the assumed distance in the bulk metal[10] and polymetallic complexes.[11] The metal–hydrogen distance is a reasonable compromise between the estimated bond lengths for terminal and edge-bridging hydride ligands in the published structures of complexes.[12] High-level molecular calculations[13] lead to 1.59 Å. The H–H distance in molecular dihydrogen is 0.74 Å.

III. General Considerations

(a) The Hydrogenation Mechanisms. Each of the successive hydrogenation steps represents the fixation of the two hydrogen atoms coming from a dihydrogen molecule on one or several platinum atoms to form Pt–H bonds characterized by a bond length of 1.6 Å. Depending on the distance between the two adsorbed hydrogen atoms, the H_2 molecule may or may not dissociate, during the adsorption process. This fundamental difference defines the two kinds of hydrogenation processes: molecular and oxidative. In the *molecular mechanism*, the H–H bond of H_2 is preserved (0.74 Å) and the reaction energy is directly related to the interactions between the orbitals of the dihydrogen molecule and those of the cluster. Let us analyze these interactions. The occupied valence metal molecular orbitals (MOs) of the clusters have energies in the range −11 to −14 eV, i.e., around −12.59 eV, the energy of the d AOs of atomic platinum. For example, they range from −11.50 to −14.47 eV in the Pt_{13} cubooctahedron and from −11.99 to −13.64 eV in the Pt_4 tetrahedron. For all clusters, the lowest unoccupied molecular orbital (LUMO) is within 1 eV above the highest occupied molecular orbital (HOMO) level. The occupied σ level of H_2 lies at −17.6 eV and the unoccupied σ^* level at +4.25 eV. As a result, the main stabilizing interaction in a molecular adsorption takes place between the σ OM of H_2 and the unoccupied MOs of the clusters. Thus, in the molecular process, the platinum acts as an acceptor species with respect to the hydrogen molecule. To get the best overlap between the σ orbital and the nearest metal unoccupied orbitals pointing toward it, the preferred orientation of the dihydrogen is a "side" one. For instance, $Pt(H_2)$ has the geometry of an isosceles triangle with a HPtH angle of 26.74°. Due to the axial symmetry of the bonding between the metal and the H_2 ligand, the rotation of the H_2 molecule around the bond axis is nearly barrier-free. *In the oxidative mechanism*, the dissociation of the H_2 molecule into two hydrogen atoms occurs. Since the energy of the 1s atomic orbital (AO) of a hydrogen atom lies at −13.6 eV, i.e., below the level of the HOMO of the cluster, it is convenient to analyze the interaction between the cluster and the two incoming hydrogen atoms by considering their 1s AOs as doubly occupied. This occupation would result from a two-electron transfer from the HOMO of the adsorbing cluster to the 1s hydrogen orbitals. Thus, formally,[14] the dissociative hydrogenation involves a reduction of the hydrogen atoms to hydride H^- and is associated with a +II oxidation step for the platinum cluster. The loss of the H_2 molecular energy must be compensated by the formation of two strong Pt–H bonds in order to get an energetically favorable process. These bonds will result from the interaction of the LUMO of the oxidized cluster and the orbitals of the hydrides. The Pt–H bonding is stronger than in the molecular adsorption because there is a drastic reduction (from 5 to 1 eV) of the energy gap between the unoccupied orbitals of the cluster and the occupied orbitals of the ligands. This reduction comes from the higher position of the orbitals of the H^- ligands with respect to those of the H_2 ligand and from the lowering of the Fermi level of the cluster by oxidation. Thus, within the present scheme, the formation of the hydrogenated clusters by both processes can be analyzed by examining the interaction of the metallic centers with ligands (H^- or H_2) characterized by doubly occupied HOMOs. This method is equivalent to considering a hydrogenation step as a Lewis acid–basic reaction.

(b) Factors Determining the Structure. To understand which factors determine the structures of the hydrogenated compounds, let us select the main ones on the basis of the dominant bond strengths. The H_2 molecular energy is ca. 8.0 eV in the EHT scheme; thus a feasible oxidative addition has to build two strong Pt–H bonds with a bond energy exceeding 4.0 eV. The cluster cohesion energy per Pt–Pt bond has been shown to be small comparatively (ca. 0.40 eV).[3] It is therefore reasonable that the position of one hydrogen ligand on the hydrogenated clusters depends more on the orientation of the other ligands than on the orientation of the metal–metal bonds. Consequently, we will analyze the hydrogenated clusters as sets of monometallic platinum complexes and we will neglect the metal–metal bonds. Within such a scheme, the adjacent complexes can share some ligands, which will impose constraints on the relative orientation of the adjacent complexes. The coordination structure of the cluster will result from these constraints.

The occupied orbitals of the hydride and H_2 ligands interact with all the valence MOs of the metal clusters which overlap significantly with them, regardless of their occupation. According to the fragment analysis, the interaction with an unoccupied metal

---

(6) Fraissard, J. P.; Ito, T.; de Mènorval, L. C., 8th International Congress on Catalysis, Berlin, 1984. Fraissard, J. P.; Ito, T.; de Mènorval, L. C.; Springuel-Huet, M. A. "Metals Microstructures in Zeolites"; Jacobs, P. A., Ed.; Elsevier: Amsterdam, 1982.

(7) Hoffmann, R. *J. Chem. Phys.* **1963**, *39*, 1397.

(8) Whangbo, M. H.; Hoffmann, R. *J. Am. Chem. Soc.* **1978**, *100*, 6093. Minot, C.; Van Hove, M.; Somorjai, G. *Surf. Sci.* **1982**, *127*, 441.

(9) (a) Hoffmann, R.; Hofmann, P. *J. Am. Chem. Soc.* **1976**, *98*, 598. Ammeter, J. H.; Burgi, H.-B.; Hoffmann, R. *J. Am. Chem. Soc.* **1978**, *100*, 3686. (b) The charge iteration procedure would lower the atomic d levels and reduce the charge transfer. For example, with the usual parameters (see Table I) the net charges of $PtH_4(H_2)_2$ are +1.012, 0.067, −0.331, and −0.308 for the platinum atom, the molecular hydrogens, and the apical and the equatorial hydrides, respectively. The total energy is −268.258 eV. The charge iteration procedure leads to following parameters (Pt 5d, −14.274 eV; 6s, −11.65 eV; 6p, −5.728 eV. H_{mol}, −15.023 eV; H_{ap}, −11.73 eV; H_{eq}, −12.45 eV) and to net charges +0.025, +0.051, −0.071, and −0.043, respectively. The total energy is −282.1548 eV. The charge iteration procedure corrects in the right direction, but in an excessive manner, the parameters. No comparison can be made between the different clusters.

(10) "Handbook of Chemistry and Physics", 55th ed.; CRC Press: Cleveland, Ohio, 1973. Wells, A. F. "Structural Inorganic Chemistry"; 3rd ed.; Oxford, University Press: London, 1962; p 84. Gallezot, P.; Bergeret, G. *J. Catal.* **1981**, *72*, 294.

(11) See: Muetterties, E. L., et al., ref 2. p 109. Longini, P.; Chini, P. *J. Am. Chem. Soc.* **1976**, *98*, 7225.

(12) From: Basch, H.; Topiol, S. *J. Chem. Phys.* **1979**, *71*, 802. Baetzold, R. *Chem. Phys.* **1979**, *38*, 313 and ref 8b.

(13) Pacchioni, G.; Koutecky, J.; Fantucci, P. *Chem. Phys. Lett.* **1982**, *92*, 486.

(14) Muetterties, E. I. *Angew. Chem., Int. Ed. Engl.* **1972**, *17*, 545. Selwood, P. W. *J. Catal.* **1976**, *42*, 148. Meakin, P.; Jesson, J. P.; Tolman, C. A. *J. Am. Chem. Soc.* **1972**, *94*, 3240.

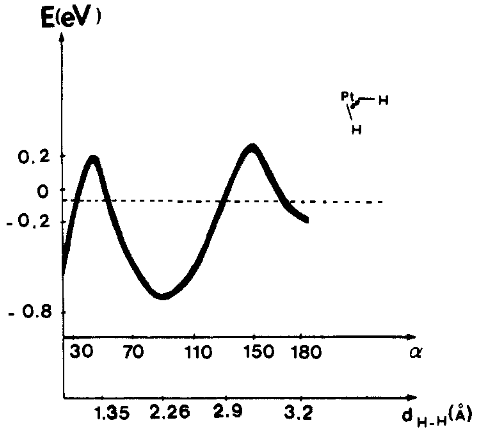

Figure 1. Energy curve of PtH_2 vs. α, the HPtH angle, or *d*, the H–H distance, for a fixed Pt–H distance of 1.6 Å.

MO is stabilizing (two-electron term) while the interaction with an occupied MO is destabilizing (four-electron term). The result is that the electron count on the metal cluster is critical in determining whether a ligand–cluster interaction is attractive or repulsive.

A nonoxidized metal atom is characterized by a set of four vacant sp^3 orbitals and by a set of five occupied d orbitals. Necessarily, one of the d orbital points at the ligand position. This generates a repulsive interaction. For an atom oxidized at the (+II) state, the d orbital which points toward the ligand becomes unoccupied. The repulsive interaction is replaced by an attractive one. So, it is possible to bind a ligand without introducing a repulsive interaction with a d orbital; a molecular hydrogenation can occur. The oxidation number of platinum is the key factor in determining whether an incoming H^- or H_2 ligand can be bound and in which direction it will be fixed. A molecular hydrogenation is never the most favorable process for a first hydrogenation step on a cluster made of Pt(0) atoms (d^{10}). The magnitude of the interaction with the sp^3-unoccupied set of orbitals is large,[15] but it is insensitive to the relative orientation of the ligands since this set is centrosymmetric. The formulae of the saturated compounds depend on the oxidation number of all the metal centers. As is well-known in coordination chemistry, the optimal number *n* of ligands (H^- or H_2) to be fixed on a platinum center is equal to the number of its vacant orbitals $m = 4 + n_{ox}/2$, where n_{ox} is the even oxidation number of the platinum atom and the optimal orientations of the ligands are in the direction of the main axis of the $n_{ox}/2$ vacant d orbitals. The best solutions for the Pt complexes are d^8 square-planar structure with four ligands and d^6 octahedral structures with six ligands.

Figure 1 shows the energy of PtH_2 as a function of the α HPtH angle and thus of the H–H distance. The curve has three minima at α = 26.74°, 90°, and 180°. That at 26.74° corresponds to a molecular addition and the two others to oxidative additions. The first minimum corresponds to a stabilization of 0.415 eV, but the highest orbital of the system has been destabilized by 0.376 eV with respect to that of the naked atom. Thus, the energy of the molecular hydrogenation on Pt^{2+} would be 1.167 eV. The energy barrier at 44° or 1.2 Å (+0.20 eV) separating the minima at 26.74° and 90° defines the border between the two types of hydrogenation mechanisms. At this point, the σ^* level lies at −12.1 eV, and electronic transfers from (to) the metal are quasiisoenergetic. Below that value, the σ^* level is vacant and the two hydrogen atoms interact favorably to form the dihydrogen molecule. Above that value, the σ^* level is occupied and the hydrogen atoms can be viewed as two independent hydrides; the platinum atom is oxidized. The 90° and 180° minima correspond to the best possibilities for the two hydrides to interact with the same d orbital; this is a requirement since one d orbital only is vacant. Any small distortion away from these angles is strongly destabilizing. The best adsorption energy (0.73 eV) takes place at 90°: the first hydrogenation which occurs on a d^{10} platinum atom is an oxidative one; it places two cis hydride ligands. The last minimum (0.19 eV) takes place at 180° (two trans ligands). The predominance of the 90° minimum over the 180° position illustrates the "cis effect", well-known in coordination chemistry. Two opposite factors determine this relative ligand orientation: the first is the antibonding interaction between the two hydrides (+0.02 eV at 180° and +0.22 eV at 90°); the second is the bonding interaction between the occupied orbitals of the hydrides and the vacant orbitals of the metal which builds up the Pt–H bonds. The magnitude of the latter factor increases sharply when the energy gap between the hydride orbitals and the metal ones is reduced by shortening the H–H distance. This factor is dominant and favors the 90° angle over the 180° orientation.

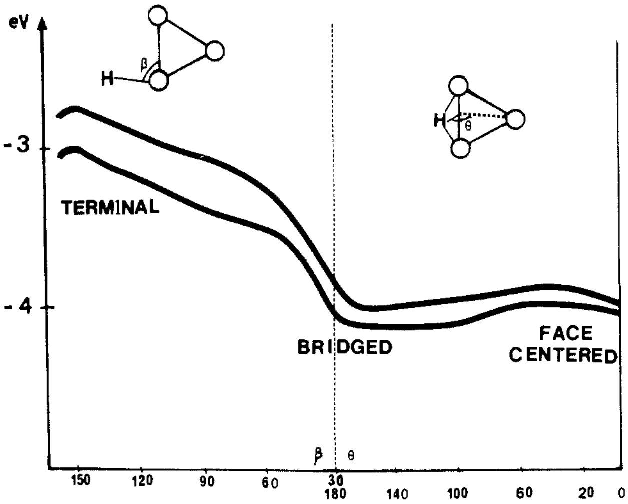

Figure 2. Stabilization energy curves of the HPt_3^- systems vs. β angle (left part) and vs. θ angle (right part). The reference system is Pt_3 + H^-. The lower curve refers to the EHT calculation and the upper one to the calculation including spin–orbit coupling with a fixed Pt–H distance of 1.60 Å between the nearest Pt and H atoms. The Pt–Pt distance is 2.77 Å.

An equivalent energy curve for the system $Pt(H_2)_2^{2+}$ is observed. In both cases, a $Pt(d^8)$ atom is bound to two Lewis base ligands, H_2 or H^-. At the lowest minimum, 100°, the mean molecular adsorption energy per H_2 molecule is 0.86 eV.[16]

The main conclusion coming from Figure 1 is that the energy of the hydrogenated cluster depends strongly on the relative orientation of the ligands. The metal–metal framework is made of the d orbitals unaffected by the ligand field. Thus, the metal–metal and metal–ligand network are deeply entwined, one being in the bisecting direction of the other.

(c) Metal–Ligand Orientation. We distinguish three kinds of positions for the hydride ligands: terminal ligands are bound to a single platinum and bridged or face-centered ligands are bound to two or three metallic atoms, respectively. In the bridged geometry, the MMH angle is 30.045°. In the face-centered geometry, the hydrogen lies at the center of a triangular Pt_3 face of a cluster with a Pt–H distance of 1.5993 Å. This value is slightly smaller than the Pt–H bond length, 1.6000 Å, that we have for the other positions. For a strict consistency with our methodology, the H ligand would have to be raised slightly above the metallic plane. We will see latter the influence of this move on the Pt_6 and Pt_{10} clusters.

The smallest Pt_n cluster for which the three kinds of ligands may be found is the equilateral-triangle Pt_3 cluster. Let us consider

---

[15] For a metal–hydrogen distance of 1.6 Å, the overlaps of the 1s hydrogen AO with the 6s (0.37), 6p (0.48) platinum orbitals are twice as large as the overlap with the 5d orbitals (0.20).

[16] The first adsorption (1.167 eV) is more stabilizing than the second one (0.553 eV) because the LUMO of Pt $(H_2)^{2+}$ lies higher in energy than the LUMO of Pt^{2+}. The adsorption energy for two H^- ligands on a d^8 platinum is 8.66 eV. If one deduces the molecular energy of the dihydrogen (7.94 eV), the oxidative hydrogenation per H_2 molecule is 0.726 eV, a value slightly inferior to the molecular adsorption energy (0.86 eV).

its interaction with a hydride ligand. In Figure 2 (left part), the energy of Pt_3H^- as a function of β, the H–Pt–Pt angle, is depicted. It is shifted by 1.09 eV on going from $\beta = 150°$ (a terminal position) to $\beta = 30.045°$ (the bridged position). The increase in stability is due to the progressive introduction of the interaction of the hydride orbital with the sp^3 orbitals of a second platinum atom. The energy level of the lowest MO, mainly located on the hydride, is lowered from −15.412 to −16.218 eV. The preferred location (bridged over terminal) does not depend on the oxidation state of the cluster, since the energy level of the Pt_3H^- HOMO (a d metal orbital) is insensitive to the value of the angle β. In Figure 2 (right part), the energy of the Pt_3H^- cluster as a function of the dihedral angle, θ, which describes the folding of the platinum–platinum-bridged hydrogen plane on the cluster face is depicted. The energy variations are small (−0.01 eV at $\theta = 135°$, +0.12 eV at $\theta = 65°$, +0.042 eV at $\theta = 0°$) as compared to those observed in the motion from the terminal to the bridged position. These variations are correlated with those of the two lowest MOs (the highest MOs remain at the same energy during the process). The lowest MO, with a main contribution from the 1s hydride orbital, is stabilized as soon as the hydride gets close to the third platinum atom, i.e., for θ smaller than 80°. The second MO with a dominant contribution from the lowest orbital of the Pt_3 cluster (an in-phase combination of d orbitals) has a small metal–hydride bonding character in the bridged geometry. It results from the balance of two opposite metal–hydride orbital mixings, an in-phase mixing with p metal orbitals, and an out-of-phase mixing with d metal orbital. When the metal–hydride orbital overlap increases during the folding to the face-centered position, the weight of the out-of-phase mixing increases. The face-centered position is therefore less stable than the bridged one. The hydrogenation at the tetrahedral site has been tested on the Pt_4 cluster. Pt_4H^- is found to be more stable when H is in the bridged position than when it is in the face-centered (+0.183 eV), the terminal (+0.208 eV), or the tetrahedral (+0.351 eV) position. So, no first adsorption step on the various studied clusters involves face-centered or tetrahedral positions. The energy difference between these positions and the bridged one is, however, small enough to make them appear in some stable polyhydrogenated clusters when the ligand fields of adjacent complexes match adequately.

IV. Results

We shall now present the detailed results of the successive hydrogenations of the clusters Pt_n (n = 1, 4, 6, 10 and 13) which are representative of the studied series Pt_1–Pt_{13} whose complete results will be reported later on.[19] However, the discussion of section V will consider the results on all the clusters. We discuss mostly the first and the last hydrogenated structures. Let us first consider the single atom "cluster" hydrogenation to set the main features of the local coordination steps of a given platinum atom in a cluster.

Pt_1. As was mentioned above, the first hydrogenation step is oxidative. It represents an energy gain of 0.73 eV whereas molecular adsorption gives only 0.42 eV. The stabilization for the oxidative addition results from the interaction between the empty atomic orbitals (one s, two p, and one d) of the metal (−10.0 to −12.6 eV) and the two occupied hydride orbitals (−13.6 eV). The charge on the metal (+0.50 ua) is large compared to the charge induced by molecular adsorption (−0.16 ua). Thus, the term of oxidative addition is justified even though the formal charge of +2 is reduced by the formation of two Pt–H strong mainly covalent bonds.

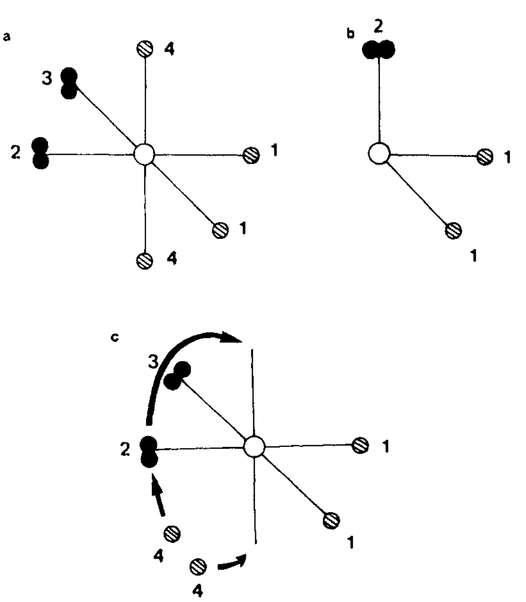

Figure 3. (a) Structure of the fully hydrogenated platinum complex $PtH_4(H_2)_2$. Numbers refer to the successive hydrogenation steps. For the corresponding energies, see Table II. Double black circles represent the H_2 ligands, hatched circles the hydride ligands, and large white circles the platinum atom. This convention will be used throughout all the figures. (b) Orthogonal $PtH_2(H_2)$ unstable structure. (c) Example of a possible reorganization from $PtH_2(H_2)_2$ to $PtH_4(H_2)_2$ during the hydrogenation process.

The PtH_2 complex with a H–Pt–H angle of 90° may be interpreted as a d^8 platinum atom bound to two hydride ligands. It has an empty $d_{x^2-y^2}$ orbital which can interact with two more ligands to generate a d^8 $PtH_2(H_2)_2$ square-planar structure where platinum is in a formal (+II) oxidation state. These two molecular adsorptions induce stabilization energies of 0.472 and 0.424 eV, respectively. For the next step, it is not possible to add a supplementary ligand without interacting with a second d orbital. Since this orbital is occupied, an oxidative step is required to get a stabilizing interaction. It leads, with an energy of 0.20 eV, to a $PtH_4(H_2)_2$ octahedral complex (Figure 3a) with a formal d^6 platinum. The two last hydrides interact with the d_{z^2} orbital of the square-planar complexe. That leads to the well-known octahedral splitting of the d orbitals (two over three) which is stable for the d^6 metal atoms. The best structure is an octahedron with four hydride ligands and two cis H_2 ligands. The trans geometry is less stable by 0.13 eV. No further hydrogenation step has been found to be exothermic. The mean adsorption energy per H_2 is 0.46 eV.

In going from the naked cluster to the saturated cluster, it is necessary to respect the order of introduction of the ligands. The oxidative addition which places the apical ligands is unfavorable if it comes too soon. As an extreme example, the molecular addition of H_2 to PtH_2 which leads to a $PtH_2(H_2)$ structure with three orthogonal bonds (Figure 3b) is endothermic by 1.48 eV though this fragment is a part of the final octahedron. In this addition, the dihydrogen molecule interacts with an occupied d orbital.

If the order of the successive hydrogenations is well-defined, no conclusion can be drawn on the mechanism of each step. As an example, the last step probably implies a reorganization of the complex. Indeed, it is unlikely that two hydrides coming from the same dihydrogen molecule could occupy trans positions in the complex. It seems more reasonable as in Figure 3c that one of

---

(17) For the naked cuboóctahedron cluster, the central atom is negatively charged. This charge (−0.19) is the sum of the s (−0.13), p (−0.13), d (+0.7) contributions. This charge is due to the population of the lowest (sp) combinations, mainly localized on the central atom. The external atoms are positively charged. This is different from the surface of a crystal which is negatively charged with respect to the bulk,[3] the difference being due to the d contribution.

(18) For the non-oxidized naked cluster, the d block orbital is completely filled in a first approach and induces no bonding. The cohesion energy comes from the polarization of this fully occupied d block by the unoccupied sp^3 block, neglected in this first approach. In the saturated structures, the metal–metal bond involves the nonbonding d orbitals of the complexes (three by center in the case of d^6 octahedra) which are still completely filled and again induce no bonding. As in the naked cluster, the metal–metal bonding comes from the polarization. Indeed, this one is smaller. It only concerns a reduced part of the d orbitals and the sp^3 orbitals of the platinum, being now involved in the metal–ligand bonding, are less available. As a general result, the metal–metal overlap population of the saturated compound is reduced by a factor of four relative to the naked compound. This reduction increases the possibility of cluster reorganization.

(19) Minot, C.; Bigot, B.; Hariti, A., to be submitted.

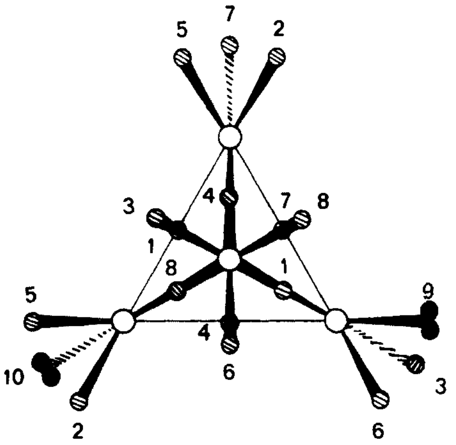

Figure 4. Saturated cluster $Pt_4H_{16}(H_2)_2$.

them occupies the position of a ligand of the planar square structure (H or H_2) by forcing it to move to an apical position.

Three main conclusions for the real clusters can be drawn from the study of a single atom: (1) The relative orientation of the ligands is of prime importance; it is determined by the symmetry of the vacant d orbitals; the angular dependence on the energy is large. (2) The stable hydrogenated structures are the planar square d^8 complex and the octahedral d^6 complex. (3) The energies of the successive hydrogenation steps are in a decreasing order with a main gap between the first hydrogenation which is oxidative and the second one. We shall next discuss whether these conclusions hold on Pt_n clusters, $n = 2–13$.

In the above sections, we described each ligand as a Lewis base interacting with a metallic center along the priviledged axis: the four directions of a square planar or the six directions of an octahedron. Within this scheme and if we assume that the hydride ligands are Lewis bases for *each metal center* (1, 2, or 3) to which they are bound, the number of bridged, b, face-centered, f, tetrahedral, t, and dihydrogen ligands, m, of the hydrogenated clusters only made of fully saturated square planar d^8 and/or octahedral d^6 complexes are linked by the general relation

$$m = 2n - 3t - 2f - b \qquad (1)$$

Pt_4. The tetrahedron is the most stable structure of the Pt_4 clusters. The first hydrogenation step places two bridged hydrides on nonadjacent Pt–Pt bonds with a large stabilization of 2.23 eV (twice the value for the fixation of a unique bridging hydride ligand on Pt_3).

The saturated compound which corresponds to the maximum of stability has the formula $Pt_4H_{16}(H_2)_2$ (see Figure 4) and may be viewed as made of four d^6 octahedral complexes. All the Pt–Pt bonds are bridged by hydride ligands. Three opposite terminal ligands on each vertex achieve the local octahedral structures. Among them, two H_2 ligands are on two different Pt centers in agreement with relation 1. Due to the bridging requirements, the orientation of the ligands (HPtH = 103.78°) does not correspond strictly to those of a regular octahedron (90°). The mean adsorption energy per H_2 is 0.74 eV. It is a significant increase by comparison with the clusters Pt_2 (0.53 eV) and Pt_3 (0.58 eV).

The second step of hydrogenation on the way from Pt_4H_2 to the saturated cluster is oxidative and introduces two terminal hydride ligands on the two platinum atoms of a bridge. They form a planar structure with the bridged hydride; the HPtH angles are close to 90°. The third step does the same for the other bridge. The associated reaction energies are respectively 0.75 and 0.65 eV. The fourth step (0.63 eV) is still an oxidative addition and fills two new nonadjacent bridges. The resulting Pt_4H_8 cluster has four equivalent d^8 platinum atoms bound to two bridged and one terminal hydrides. Four successive molecular hydrogenations, with an averaged energy of 0.40 eV (a value similar to the one observed on Pt_1), lead to a C_{2v} cluster $Pt_4H_8(H_2)_4$ made of four equivalent d^8 platinums surrounded by four ligands in a square-planar arrangement. However, this stable cluster is not the most stable isomer. Instead of four H_2 ligands, four hydride ligands are introduced by two oxidative steps (0.76 and 0.78 eV) and two high-lying orbitals of the Pt_4 cluster are emptied. It opens the way to the formation of a cluster with d^6 platinum atoms. The preferred hydrogenation steps do not complete the planar square environment before introducing apical ligands, contrary to the observation reported on Pt_1 and also true on Pt_2 and Pt_3. The reason is that now the d_{z^2} occupied orbitals of the different platinum atoms overlap each other significantly (the z axis refers to the direction normal to the plane of the squares in the complexes). As a result the upper antibonding d_{z^2} levels lie high in energy. Therefore, it is better to empty these levels by oxidative hydrogenations than to complete the d^8 planar square coordination of the platinum atoms by molecular additions. After these steps, two oxidative additions (0.52 and 0.33 eV) place a bridging ligand and a terminal ligand on the same center simultaneously to generate two platinum atoms with a d^6 octahedral environment; molecular hydrogenations (0.42 and 0.39 eV) on the last two platinums lead to the above-described structure $Pt_4H_{16}(H_2)_2$. These last values are equivalent to those observed above for the formation of a d^6 octahedral or d^8 planar square coordination by molecular addition. This performance reinforces the local scheme consideration used in the present study.

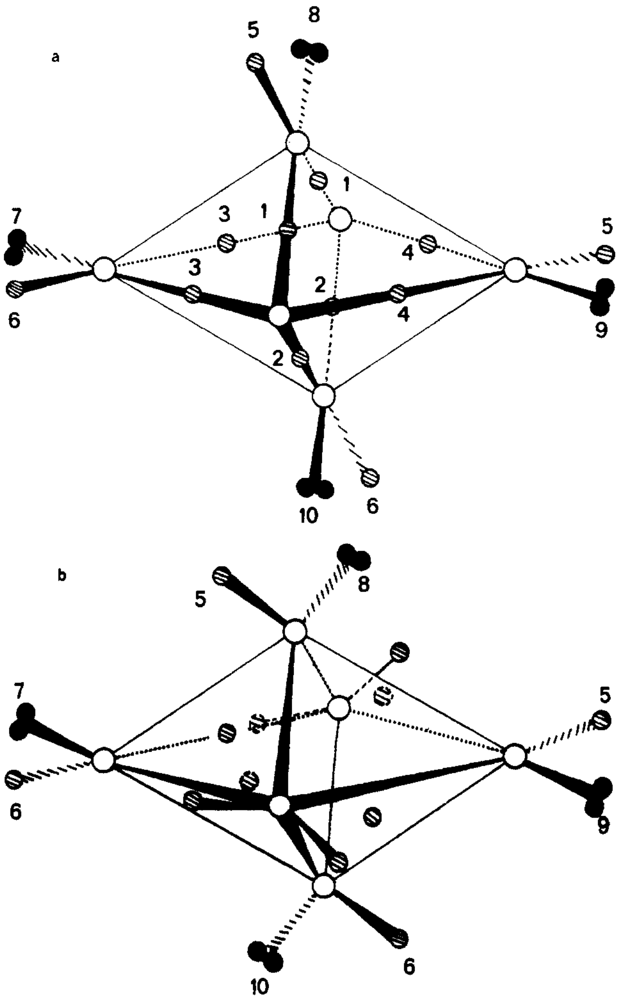

Figure 5. (a) Saturated fully bridged cluster $Pt_6H_{12}(H_2)_4$. (b) Saturated face-centered cluster $Pt_6H_{12}(H_2)_4$ (the most stable isomer). The nonnumbered positions correspond to the 1–4 hydrides which move from their position in part a.

Pt_6. The best Pt_6 cluster is an octahedron. The first hydrogenation step is oxidative and places two bridging hydride ligands on adjacent Pt–Pt bonds in a planar arrangement. Its energy is 1.45 eV. The bridging of all the metal–metal bonds does not allow the formation of undistorted local planar squares or octahedra (the C_{2h} $Pt_6H_{12}(H_2)_4$ cluster (See Figure 5a) made of d^8 platinum complexes is less stable than the best isomer by 0.64 eV). On the contrary, four face-centered hydrides are well suited to build local planar square complexes since the face-centered hydrides located on two nonadjacent faces define H–Pt–H angles (70.5°) which can be considered, in a first approximation, as an acceptable distortion from 90°. It is easily feasible to add on this vertex two terminal ligands to complete a slightly distorted planar square coordination. This construction generates a d^8 structure of formula $Pt_6H_{12}(H_2)_4$ of D_{2d} symmetry which is the saturated stable compound (Figure 5b). The introduction of two new terminal hydride ligands in directions perpendicular to the plane of the planar square complexes would lead to a structure $Pt_6H_{24}(H_2)_4$ made of six d^6 platinum octahedral complexes. Although the electronic and geometric requirements of the local complexes are fulfilled, this structure is unstable for steric reasons (too short H–H and Pt–H distances between nonbonded atoms).

To move the hydrides slightly out of the triangular faces decreases the angular distortions in the $Pt_6H_{12}(H_2)_4$ structures with centered faces. The stabilization is increased by 0.70 eV when the hydrides are moved 0.24 Å above the triangular faces. The Pt–H bond length is increased from 1.599 to 1.623 Å and the H–Pt–H angle from 70.5 to 90.0°. This favorable move is at variance with what is observed for a hydrogen atom when only a face is involved (see Figure 2) and illustrates again the importance of the relative angular orientation of the ligands around a metallic center.

The first hydrogenation steps do not anticipate the final structure. Indeed, the first four hydrogenation steps (1.45, 0.79, 0.57, 0.65 eV) place eight bridging hydrides around two of the three Pt_4 planar square fragments in which the Pt_6 octahedron can be decomposed. One square is completed first by bridging two of its opposite edges before starting on a second one. Next, there is a progressive switch from bridged positions to centred ones. The fifth hydrogenation step (0.78 eV) involves a first location change for the hydrogen atoms already adsorbed on the cluster. Indeed, the best Pt_6H_{10} isomer has a centered triangular face, six terminal hydrides on the platinum atoms of this face, and three bridged edges on the triangular face parallel to the first one. The next step (0.85 eV) induces a new structure change to generate a Pt_6H_{12} isomer with 4 nonadjacent face-centered hydrides and eight terminal hydride ligands in positions identical with those found for the saturated structure. This compound is generated by four successive molecular hydrogenation steps (0.53, 0.49, 0.47, 0.47 eV) to complete the planar square coordination of the equatorial d^8 platinum atoms. No further hydrogenation has been found to be exothermic. The mean adsorption energy per H_2 is 0.70 eV. It is less than what has been found for Pt_5 (0.76 eV). For the first time, the mean adsorption energy at saturation does not increase with the cluster size.

Pt_{10}. The most stable Pt_{10} isomer has a D_{2h} symmetry. It can be described either as the parallel superposition of two Pt_5 trapeza or as two adjacent octahedra sharing a common edge. It will also be referred to as composed of a Pt_6 equatorial rectangle with a pair of atoms located "above" and "below" this equatorial plane. The first hydrogenation step (1.27 eV) places two bridging hydrides in the equatorial plane, along either the long or the short sides of the rectangle. The structure of the saturated compound $Pt_{10}H_{28}(H_2)_2$ (Figure 6a) is derived from the saturated structure of the Pt_6 octahedral cluster. It has eight face-centered hydrides, four on each octahedron; two of them are inside the cluster. It is the first example of ligands located within the volume of the cluster. The face-centered hydrides are slightly out of the faces and generate a local D_{2d} symmetry for each octahedron as for Pt_6. The hydrogenated cluster keeps an inversion center of symmetry. The structure is completed with terminal or bridging hydrides and dihydrogen ligands. Only the Pt–Pt bonds of each couple of platinum atoms located "above" and "below" the equatorial plane are bridged. In each such couple, one atom has d^8 character with a slightly distorted square-planar coordination and the other has d^6 character with a slightly distorted octahedral coordination. The four atoms located at the corner of the equatorial plane have two terminal ligands and have d^8 character with a square-planar coordination. The last two atoms located at the middle of the long side of the rectangle have two terminal ligands and have d^6 character with an octahedral coordination. The two H_2 ligands which are introduced in the last step of hydrogenation are located at two opposite corners of the rectangle. The good match of the local complexes is illustrated by the mean adsorption energy per H_2 (0.58 eV). The first steps up to $Pt_{10}H_{14}$ (Figure 6b) place bridging ligands with reaction enthalpies decreasing regularly from 1.27 to 0.33 eV. The next step (0.94 eV) induces a move of six hydrogen atoms already fixed in the bridging positions to face-centered positions. The last two face-centered hydrides of the final structure are those internal to the cluster; they are only introduced during the 15th step. In-between, terminal ligands are introduced. The last step introduces two molecular ligands in sites which were previously occupied by hydrides. It supposes a reorganization of the ligands, including at least a recombination of two hydrides.

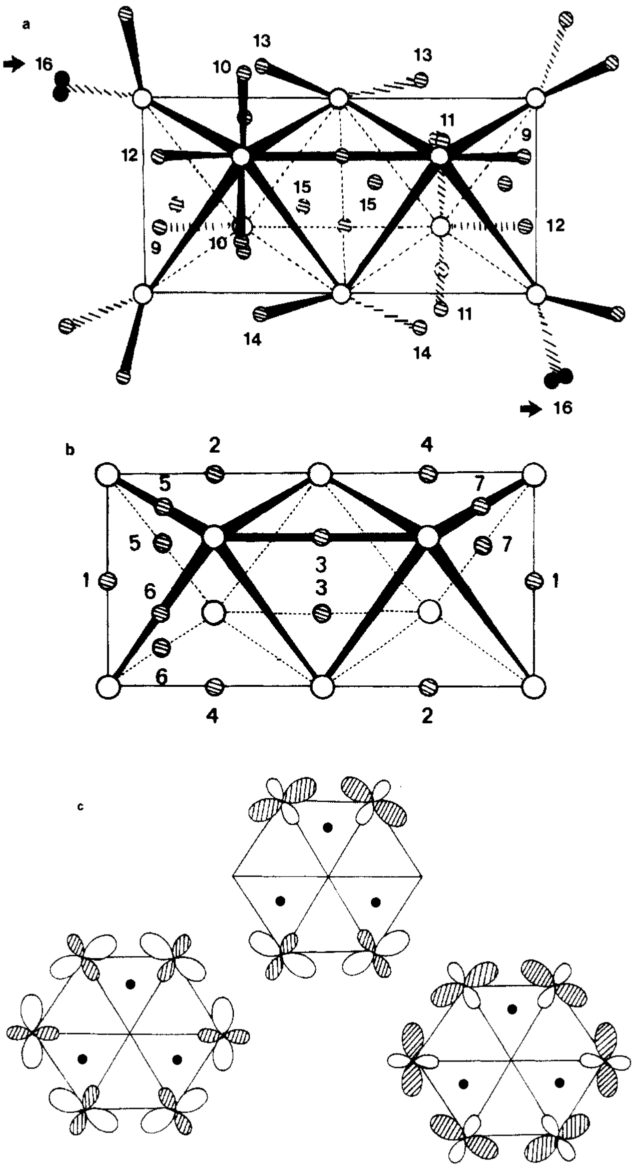

Figure 6. (a) Saturated structure of $Pt_{10}H_{28}(H_2)_2$. (b) Structure of $Pt_{10}H_{14}$, the intermediate structure with bridging ligands which will move to face-centered positions to generate the saturated cluster. (c) The three MOs involved in the cooperative effect for the first hydrogenations of the Pt_{10} cluster of C_{3v} symmetry.

We also considered the C_{3v} cluster made of the parallel superposition of a Pt_7 centered hexagon and a Pt_3 triangle. It can be viewed as a incomplete cubooctahedron (Pt_{13}) with three adjacent atoms removed. It is less stable by 0.30 eV than the structure studied above. The first three hydrogenation steps place bridges on all the hexagon edges. They occur with enthalpies of *increasing value* (1.50, 1.75, 2.07 eV). It is a striking result compared with all the previous observations. It can be interpreted as associated with a *cooperative effect* which occurs when successive hydrogenation steps involve a common set of MOs of the purely metallic cluster. Such an effect explains that the third hydrogenation of Pt_3 is more exothermic than the second one. The structure $Pt_{10}H_6$, when in the equatorial hexagonal Pt_7 pattern, has in-plane bridging ligands on all its external bonds. The six hydride ligands interact with three MOs of the cluster only (the a and e *in-phase* combinations of the $d_{x^2-y^2}$; x refers to the radial direction of the hexagon and y to its in-plane perpendicular direction—see Figure 6c). In the first hydrogenation step, the two introduced hydrides interact dominantly with one MO of the set (the empty one) but cannot avoid some repulsive interactions with the two MOs which remain occupied. In the second step, a second MO is emptied. This allows the favorable introduction of two new ligands but also reduces the repulsive interactions since only one MO of the set remains occupied. The third step repeats and emphasizes the process since no repulsive interaction remains, the three interacting MOs being vacant. The next steps involve other MOs and therefore show no cooperative effect.

The results $Pt_{10}H_6$ isomer is 1.56 eV *more stable* than the isomer derived from the bioctahedral Pt_{10} cluster. The next step bridges two other edges and is associated with an enthalpy of 1.12 eV. There is no cooperative effect in this case. The eleven further successive hydrogention steps lead to a structure with 18 bridging hydride ligands (on all the 15 bonds which do not pertain to the hexagonal face first and at the end on three bonds of this face) and 12 terminal hydride ligands on all the peripherical platinum atoms of the hexagonal face to generate a $Pt_{10}H_{30}$ structure. It is 3.86 eV more stable than the equivalent isomer in the dioctahedron series and has a mean adsorption energy per H_2 of 0.87 eV. This is the highest value found for a saturated cluster. This structure can be considered as being made of six d^6 octahedral complexes and three d^8 square planar complexes in near optimal geometry. The last platinum atom is located at the center of the hexagon and would be a d^{10} center with three ligands. The above results clearly show that the most stable purely metallic clusters do not necessarily lead to the structure of the best hydrogenated compounds. The hydrogenations can induce strong change in the cluster structure and even split apart the larger clusters as will be shown below.

Pt_{13}. The most stable Pt_{13} cluster can be considered as the parallel superposition of a Pt_7 centered hexagon and a Pt_6 triangle. The first hydrogenation bridges two of the six bonds connecting the vertices of the Pt_6 triangle (the sites of lowest coordination) to the vertices of the Pt_7 hexagon. Bridging the edges of the hexagon first is quasi-isoenergetic (smaller by 0.013 eV only). This would be the precursor of the following structures. The $Pt_{13}H_4$ and $Pt_{13}H_6$ structures have bridging hydride ligands all around the Pt_7 hexagon. The first three hydrogenation steps are similar to those observed for Pt_{12}. These first hydrogenations illustrate as in Pt_{10} the cooperative phenomenon (the successive adsorption energies are in increasing order: 1.35, 1.65, 1.90 eV). The fourth step (0.82 eV) which places bridging hydrides on the edges of the Pt_6 triangle has a reduced energy. It does not participate to any cooperative effect. The saturated structure is $Pt_{13}H_{34}$ (Figure 7a). Nine hydride ligands are face-centered, one is in the central tetrahedral site, and two are bridging the edges of the triangular faces. The formula is made of an ensemble of nearly-non-distorted local octahedral or square-planar complexes with two uncomplete octahedra and of one bipyramidal complex (the center of the hexagon). The bipyramidal complex is stable with a d^4 electron count. This requires the modification of expression 1 into

$$m = 3t - 2f - b - c \qquad (1')$$

(see Table IV). The introduction of two hydride ligands on the uncomplete octahedra is found to be slightly endothermic (−0.16 eV). The mean energy per H_2 molecule is 0.70 eV.

$Pt_{13}H_{34}$ represents the first example where the upper combinations of the locally nonbonding d atomic orbitals (here mainly the $d_{x^2-y^2}$ and d_{xy} orbitals of the atom at the center of the hexagon) are slightly above the lower combinations of the d atomic orbitals raised by the local ligand field (here the antibonding MOs of the hexagonal ring). The energy gap associated with the stability of the local complexes is no longer apparent at the molecular level. In the present case, this situation does not, however, affect the general relation between the local geometry requirements and the stability of the system. It reinforces the Pt–Pt bonding around the hexagonal ring (their overlap population is 0.12, a value twice as large as any other Pt–Pt term) while it weakens some Pt–H bondings in the hexagonal face (the overlap population is 0.21 while it is 0.28 for the others).

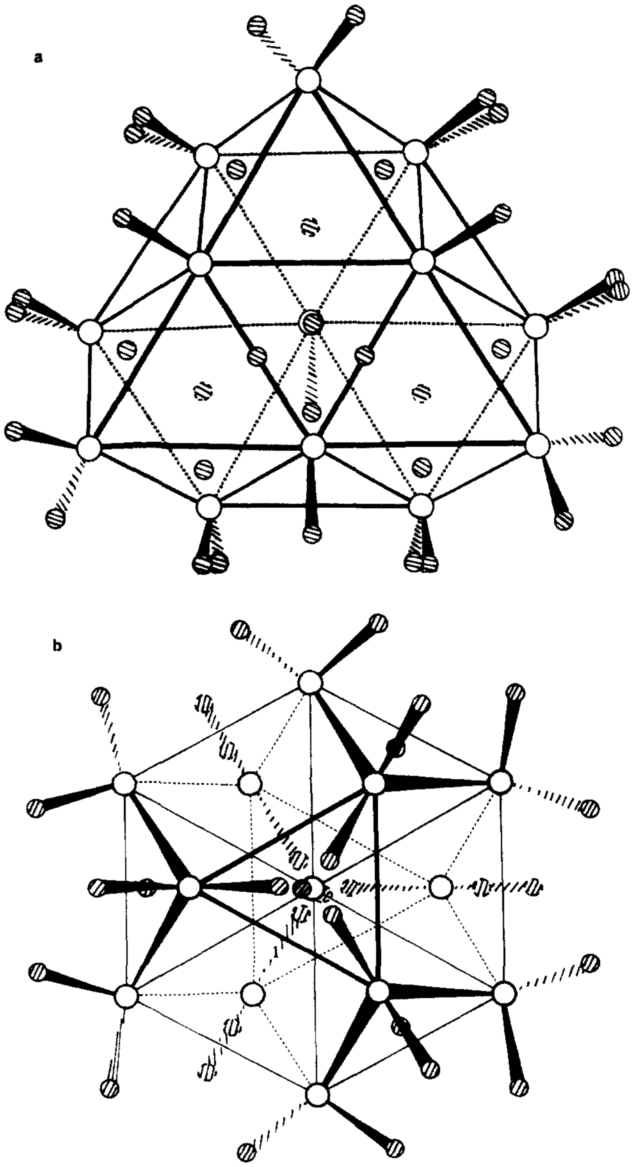

Figure 7. (a) Structure of the saturated $Pt_{13}H_{38}$ cluster made of a Pt_7 hexagonal layer and a Pt_6 triangular parallel layer. (b) Structure of the saturated $Pt_{13}H_{32}$ cluster made of a metal cubooctahedron.

The hydrogenation of the Pt_{13} cubooctahedron has been studied too. It can be considered as being made of three parallel layers, an equatorial Pt_7 hexagonal, and two Pt_3 triangular ones. The naked cubooctahedron is 0.25 eV above the most stable Pt_{13} isomer. As for the other structure, a cooperative effect is observed for the first three steps which bridged too the edges of the hexagonal layers (1.31, 1.54, 2.16 eV). The saturated structure is $Pt_{13}H_{32}$ (Figure 7b). All the triangular faces are centered and all the external platinum atoms have two terminal ligands. Its mean adsorption energy per H_2 is 0.63 eV. It makes this hydrogenated cluster less stable than the compound of Figure 7a by 1.45 eV. For the first time, there is an internal platinum atom. All the ligands on the surface atoms are hydrides, whereas eight H_2 ligands may be expected by counting the square planar coordinated surface atoms as d^8. By keeping this assumption, the central atom becomes a highly oxidized d^2 platinum. Calculations

Table II. Energies EHT and EHT-SO of the Pt_nH_{2m} Clusters and Cumulated Hydrogenation Energies δE_{EHT} and $\delta E_{EHT\text{-}SO}$ of the Pt_n Clusters[a]

n	m	EHT	EHT-SO	δE_{EHT}	$\delta E_{EHT\text{-}SO}$
1	0	125.900	125.900	0.73	1.06
	4	268.258	268.586	1.823	2.151
2	0	252.232	252.320	1.43	1.56
	6	466.245	467.010	3.211	3.888
3	0	378.863	379.260	2.14	2.24
	9	700.303	701.103	5.237	5.640
4	0	506.056	507.107	2.23	1.85
	10	864.866	866.318	7.473	7.874
5	0	633.529	634.716	1.74	1.55
	11	1028.343	1030.253	8.343	9.066
6	0	761.096	762.372	1.45	1.13
	10	1119.505	1121.019	7.072	7.310
7	0	888.269	889.697	1.48	1.46
	11	1282.511	1284.515	7.775	8.347
8	0	1015.395	1016.950	1.40	1.48
	13	1480.923	1483.732	8.790	10.044
9	0	1142.900	1144.565	1.15	1.14
	17	1748.978	1751.948	8.805	10.110
10	0	1269.979	1272.049	1.27	1.22
	16	1841.404	1844.420	9.286	10.232
11	0	1397.019	1399.527	1.50	1.25
	17	2004.442	2007.922	10.150	11.122
12	0	1524.428	1527.018	1.40	1.51
	18	2167.473	2171.671	10.638	12.246
13	0	1651.785	1654.844	1.45	1.24
	17	2260.943	2265.276	11.885	13.159

[a] The complete results are available on request.

Table III. Calculated Energy Data on Infinite Systems[a]

	energy	adsorption energy per H_2
three layers	-383.1216	
coverage $\theta = {}^1/_3$		
top	-1167.3006	0.740
bridged	-1167.4307	0.998
hollow 3-3	-1167.3628	0.862
coverage $\theta = 1$		
top position	-400.9282	0.480
bridged	-401.0013	0.626
threefold 3-1	-400.9128	0.449
threefold 3-3	-401.0253	0.674
insertion $\theta = 1$		
tetrahedral sites	-400.5648	-0.247
(on the 1st layer)[b]		
top	-400.5772	-0.223
bridged	-400.6457	-0.086
(on the 2nd layer)[c]		
threefold	-400.6693	-0.038
bridged	-400.4052	-0.567
coverage $\theta = 2$		
molecular adsorption of H_2		
top orientation 1*	-418.0333	-0.222
top orientation 2*	-417.9636	-0.292
bridged	-417.4681	-0.787
threefold	-417.5621	-0.693
oxidative adsorption		
threefold 3-1 + 3-3	-418.2311	-0.024
threefold 3-1 + top	-418.4402	0.185
threefold 3-3 + top	-418.4975	0.242
bridges	-418.2725	0.017
two terminals (H-Pt-H 40°)	-417.0128	-1.243
threefold 3-3 + top internal	-418.1559	-0.099
threefold (1st and 2nd layer)	-418.2899	0.035
coverage $\theta = 3$		
threefold + top	-435.3634	-0.306

[a] Adsorption energies are positive when exothermic. (*): For the molecular adsorption with $\theta = 2$, the H_2 axis bisects the Pt-Pt-Pt bond angle in the first orientation and it eclipses the Pt-Pt bonds in the second one. [b] Oriented toward the inside. [c] Oriented toward the outside.

confirm this picture since the charge on the central atom is +2.24 while it is -0.19 for the naked cluster[17] and +0.54 for the external platinum atoms of the hydrogenated structure.

The (111) Pt Surface. Results of tight-binding calculations on hydrogen adsorption above a (111) platinum surface are listed in Table III. In these calculations, the same parameters have been used as in the cluster study. Different coverages of the surface (number of H atoms per surface Pt atom) of a three-layer slab have been considered ($\theta = {}^1/_3$, 1, 2, and 3). The different sites which have been studied are the top (terminal), bridging, and threefold (face centered) sites. The unit cell is either $\sqrt{3}\,\sqrt{3}R30°$ or p1×p1. For $\theta = {}^1/_3$, the best calculated site is the bridged one (0.98 eV per H_2). This result is consistent with the observation made on clusters that the first hydrogenations took place on the bridged sites. For $\theta = 1$ (one hydrogen atom per platinum atom on the surface), the best location (0.67 eV per H_2) is a threefold 3-3 site with a hole in the layer beneath. Similarly, threefold sites and terminal sites have been found on clusters for large coverages. The bridged site remains close in energy (0.63 eV). The insertion of hydrogen atoms in the metal bulk just below the surface is repulsive, whatever their location is. For $\theta = 2$, the best arrangement (0.242 eV per H_2) is made of a hydrogen on the threefold 3-3 sites together with a hydrogen on the top sites. The transformation $\theta = 1 \rightarrow \theta = 2$ is slightly endothermic (-0.19 eV per H_2). All the studied molecular adsorptions are found to be repulsive (from -0.44 eV for a top position to -1.57 eV for a bridged position). For $\theta = 3$, filling of the two holes plus the top site locations leads to a repulsion (-1.133 eV relative to $\theta = 1$ and -0.46 eV relative to the complete desorption).

These results which show that a coverage of $\theta = 1$ is energetically favorable while an increase of adsorption up to $\theta = 2$ is computed to be slightly endothermic would suggest that the saturation should take place between these two values. This conclusion must be tempered if the 6p atomic levels of the platinum atom were shifted by 1 eV with respect to the classical parameters used in coordination chemistry as is done for the 6s atomic levels in order to reproduce adequately the bulk band structure. If this were done, the hydrogen adsorption energies would be slightly increased and $\theta = 2$ may then appear as a possible adsorption rate.

V. Discussion

(a) The First Hydrogenation Step. In Figure 8, the energies of first hydrogenation step as a function of the cluster size are reported. There is a peak for Pt_4 at the EHT level and for Pt_3 when SO coupling is taken into account. It suggests that the first hydrogenation step of the small clusters is selective according to the cluster size. It would allow the interpretation of the plateaux of hydrogenations found by Xe NMR[6] as titrations of the most reactive species in a mixture of clusters of different sizes. As has been emphasized in section III, the first hydrogenations of all the studied clusters and on the (111)*fcc* surfaces at low coverage are oxidative and always involve bridged sites. The bridged bonds are found to be either adjacent (n = 3, 5, 7, 8, 9, and 11) or nonadjacent (n = 4, 6, 10, 12, and 13) for the various Pt_n clusters.

As in the discussion of Pt_3H^- (see section III), two factors control the relative preferential positions of the hydrides: the interactions of the hydride orbitals with the sp^3 and d orbitals of the platinum atoms, respectively.

For the first factor, the larger the number of platinum atoms to which the hydrides are bound the better the bonding. This determines the predominance of the bridged site over the terminal site and leads to nonadjacent bridging ligands for the first hydrogenation steps.

As the cluster size increases up to Pt_4, the energy of the lowest "sp^3" MO progressively decreases, but it remains unoccupied, and

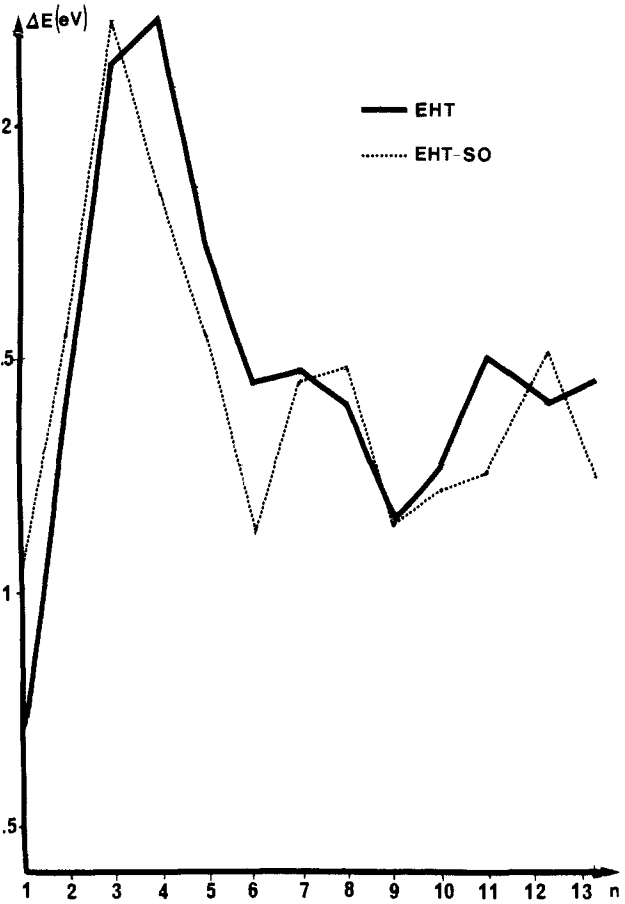

Figure 8. Stabilization energies associated with the first hydrogenation step for the clusters Pt_n, $n = 1$ to 13. The upper curve is relative to the simple EHT calculations and the lower one to the calculations which include the spin-orbit interaction.

its interaction with the hydride orbital is increased. Beyond Pt_4, an increasing portion of the "sp^3 MOs" is occupied. It gives a contribution to the metal–metal bonding and thus to the cohesion energy of the naked cluster but is no longer available for favorable ligand interaction. Worse, this occupation leads to a partial repulsion of the sp^3 set with the hydride orbitals. This explains why the best hydrogenation takes place with Pt_4 (see Figure 8).

The repulsive interaction of the d orbitals with the hydride ligands has different consequences. To avoid repulsion, the ligands must interact together selectively with the few unoccupied d MOS which have been emptied by oxidation. Contrary to the previous factor, the present one favors low coordination. It is responsible for the bridging coordination instead of the face-centered one (see section IIIc), and in most cases it would impose the first two bridging hydrides to be on adjacent bonds. However, if, for symmetry reasons, the two hydrides can interact with one unoccupied MO delocalized on several atoms, without interacting with the occupied MOs, nonadjacent bridging will be observed. This possibility of concentrating the interaction mostly on one AO (case of adjacent hydrides) or a small number of MOs is at the origin of what we called the cooperative effect (see discussion on Pt_{10}).

Let us now analyze whether the first hydrogenation takes place on the sites of high or low coordination, when both possibilities exist. In this section, every Pt–Pt bond is labeled according to the coordination number of the platinum atoms. For example, a Pt–Pt bond of the Pt_4 tetrahedron would be labeled (3,3). For trigonal-bipyramid Pt_5, the difference between the axial (4,3) and the equatorial bridging (4,4), though it is small (<0.18 eV), favors the diaxial bridging, i.e., the sites of lowest coordination. For pentagonal-bipyramid Pt_7 and its capped homologue Pt_8, the diequatorial (4,4) bridging is observed. It corresponds to the lowest coordination sites. For Pt_8, the sites (5,3) which have the same low coordination become occupied with the second hydrogenation step. This order ((4,4) better than (3,5)) suggests that with equivalent sums of coordination numbers (8), the bond most likely to be bridged first has the smallest difference between the coordination of the two atoms. To avoid involving a center with a high number of coordination is the determining factor. For Pt_9, Pt_{10}, Pt_{11}, and Pt_{12}, whose structures are described in ref 3, the first hydrogenations again concern the sites of lowest coordinations: (4,5) for Pt_9, (4,4) for Pt_{10}, (3,5) for Pt_{11}, and (4,5) for Pt_{12}. In Pt_{13}, the coordination of the atoms ranges from 4 to 9. The first hydrogenation steps on sites (4,5), 1.35 eV, or on sites (5,5) (around the hexagonal ring), 1.34 eV, are nearly isoenergetic. For all these examples, the lowest coordination sites are to be bridged first. The sum of the coordination numbers for the bridged bonds not only determines the position of the first hydrides but also influences the hydrogenation energy. The energy value for Pt_9 (1.08 eV), the smallest one in the series Pt_6–Pt_{11}, is associated with a sum of 18 while for all the other clusters the sum is 16. The reduction in energy between Pt_{11} and Pt_{12} (see Figure 8) is associated with an increase by two of the sum.

Hydrogenation on a surface at low coverage is equivalent to the first hydrogenation step for the clusters. In both cases, the bridged sites are hydrogenated first and the face-centered site (hollow site) appears at larger coverages. The surface reaction energy (0.98 eV) is significantly smaller than that of all the studied clusters by more than 0.5 eV. Atoms on a (111) surface have a coordination number of 9. Thus, small clusters are expected to be more active in an oxidative process than a metal surface. The large values encountered for clusters are related to the existence of edges. It is worth noting that the 0.98-eV value is similar to the values calculated for the perpendicular bridging of two hydrides on the Pt_7 hexagonal face of Pt_{13}.

(b) Successive Hydrogenations. In most cases, the successive hydrogenation steps occur with energies of decreasing magnitude (see Figure 9). The exceptions are usually easily understandable. They occur when there is a structural change, a cooperative effect, or when it is impossible to empty a d orbital in an appropriate direction without creating a simultaneous repulsion on a neighbor center. Some of the minor oscillations in the successive energy adsorptions probably have no physical meaning and are expected to disappear with an extensive optimization of the intermediate geometries.

The first hydrogenation steps always involve bridging ligands. The face-centered ligands come, for the first time, at the fifth step of the hydrogenation of the Pt_6 cluster. They are located within the metal volume, for the first time, in the cluster Pt_{10}. The first tetrahedral site is found for the Pt_{12} cluster.

Octahedral environment becomes more and more difficult to obtain on large clusters, and the number of ligands per platinum atom decreases. Up to Pt_5 all the platinum atoms are d^6 centers of slightly distorted octahedral complexes. For Pt_6 and above, an increasing number of platinum atoms are d^8 in a square-planar environment. For Pt_7, Pt_8, and Pt_{11} other ligand fields have to be considered on the platinum atoms of high coordination. The number of hydrogens per platinum atom in the saturated cluster decreases with the cluster size (see Table IV), except for Pt_9 which leads to a remarkably stable saturated compound (see Figure 9). Saturation of the clusters up to Pt_{11} involves some molecular additions. Their number m is determined by the formulae 1 or 1 bis (see section IV and Table IV). For Pt_{13}, the highest levels of the naked cluster are emptied by extra oxidative hydrogenations. A striking example is the hydrogenation of the cubooctahedron since the central atom has no hydride ligand but is more oxidized than any surface platinum atom.

(c) Spin–Orbit Influence. The curves with and without spin–orbit coupling for PtH^- are parallel (Figure 3). We may conclude from this result that spin–orbit coupling (SO) does not modify the preferred site of adsorption. Let us now consider the isolated atom Pt. The stabilization brought by the SO term increases with the depopulation of the d orbitals. The formation of PtH_2 from a formal d^8 platinum atom and two hydride ligands is more stabilizing at the EHT-SO level (1.06 eV) than at the simple EHT level (0.73 eV) while the introduction of the spin-coupling terms has the reverse effect for the interaction of a d^{10} Pt atom with

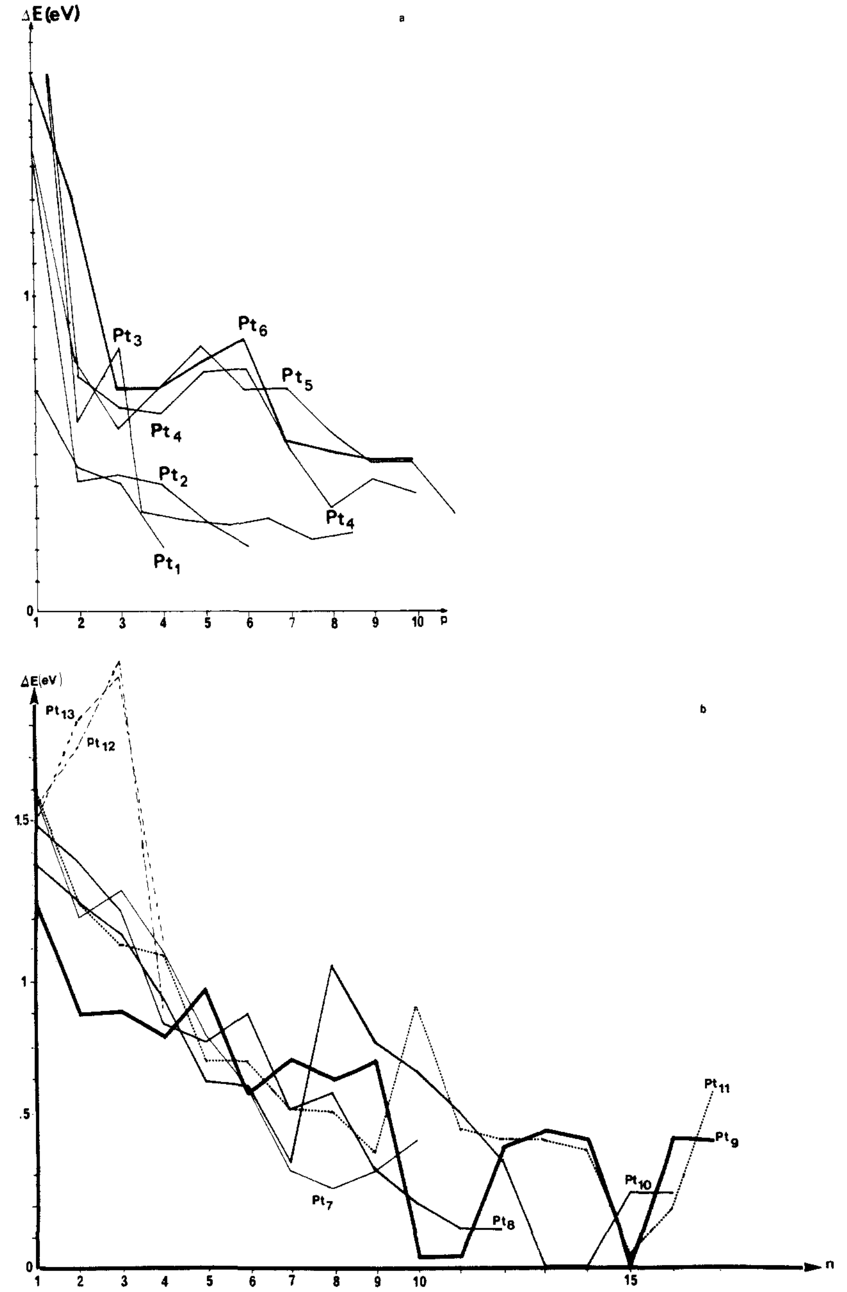

Figure 9. Stabilization energies of the successive hydrogenation steps up to saturation of the clusters Pt_n: $n = 1-6$ (a), $n = 7-13$ (b).

Table IV. Calculation of the Number of Molecular Ligands According to Formula 1′ for the Most Stable Saturated Clusters[a]

n	t	f	b	c	$2n - 3t - 2f - b - c$	n_H
1	0	0	0	0	2	8.00
2	0	0	2	0	2	6.00
3	0	0	3	0	3	6.00
4	0	0	6	0	2	5.00
5	0	0	9	0	1	4.40
6	0	4	0	0	4	3.30
7	0	0	12	2	0	3.14
8	0	0	15	1	0	3.25
9	0	8	0	0	2	3.78
10	0	8	2	0	2	3.20
11	0	9	3	0	1	3.09
12	1	7	4	3	0	3.00
13	1	9	2	3	0	2.46

[a] n_H is the number of hydrogen atom per platinum atom for these clusters.

a dihydrogen molecule. Indeed, molecular hydrogenations increase the symmetry constraint on the mixing of the d AOs without removing electrons from the d levels destabilized by the SO coupling. For the second and the third hydrogenation steps, the introduction of the SO term reduces the adsorption energy by 0.07 eV while it increases it by 0.14 eV for the fourth step which is oxidative. As a result, the saturated structure $PtH_4(H_2)_2$ has a stabilization energy larger (0.328 eV) at the EHT-SO level than at the simple EHT level. For clusters of increasing size, the gain observed with the SO contribution for the oxidative hydrogenations decreases rapidly and becomes negative for Pt_4 and larger clusters. The SO contributions to the first hydrogenations of the Pt_1–Pt_6 clusters are +0.33, +0.13, +0.10, −0.38, −0.19, −0.32, eV, respectively. As a consequence, the energies of the first hydrogenation step of the smallest clusters are increased by the SO contribution while those of the largest clusters are reduced. Thus, the SO coupling favors the hydrogenation of the small clusters and for a same cluster the first hydrogenation steps over the following ones. The peak which occurred for Pt_4 at the EHT level is shifted to Pt_3 at the EHT-SO level (see Figure 8).

(d) Relative Stability of Saturated Clusters. It has already been pointed out that the metal–ligand interactions prevailed over the metal–metal interactions.[18] This has two consequences on the metallic network when successive hydrogenations occur: a possibility of reorganization or of fragmentation. In various cases

Table V. Energies Corresponding to the Fragmentation of the Saturated Clusters into Fully Hydrogenated Fragments[a]

reaction	energy	*a*/*b*
$PtH_4(H_2)_2$		1.82/1.82
$Pt_2H_8(H_2)_2 + 2H_2 \rightarrow 2PtH_4(H_2)_2$	+0.000	1.61/1.82
$Pt_3H_{12}(H_2)_3 + 3H_2 \rightarrow Pt_2H_8(H_2)_2 + PtH_4(H_2)_2$	+0.868	1.75/2.13
$Pt_4H_{16}(H_2)_2 + 4H_2 \rightarrow Pt_3H_{12}(H_2)_3 + PtH_4(H_2)_2$	+1.765	1.87/2.48
$Pt_4H_{16}(H_2)_2 + 2H_2 \rightarrow 2Pt_2H_8(H_2)_2$	+2.633	
$Pt_5H_{20}(H_2) + 3H_2 \rightarrow Pt_4H_{16}(H_2)_2 + PtH_4(H_2)_2$	+0.649	1.67/2.47
$Pt_5H_{20}(H_2) + 4H_2 \rightarrow Pt_3H_{12}(H_2)_3 + Pt_2H_8(H_2)_2$	+2.415	
$Pt_6H_{12}(H_2)_4 + 5H_2 \rightarrow Pt_5H_{20}(H_2) + PtH_4(H_2)_2$	−1.498	1.17/2.13
$Pt_6H_{12}(H_2)_4 + 6H_2 \rightarrow Pt_4H_{16}(H_2)_2 + Pt_2H_8(H_2)_2$	−0.804	
$Pt_6H_{12}(H_2)_4 + 8H_2 \rightarrow 2Pt_3H_{12}(H_2)_3$	+0.050	
$Pt_7H_{22} + 8H_2 \rightarrow Pt_4H_{16}(H_2)_2 + Pt_3H_{12}(H_2)_3$	−1.646	1.10/2.10
$Pt_7H_{22} + 6H_2 \rightarrow Pt_5H_{20}(H_2) + Pt_2H_8(H_2)_2$	−1.333	
$Pt_8H_{26} + 7H_2 \rightarrow 2Pt_4H_{16}(H_2)_2$	−2.966	1.09/2.11
$Pt_8H_{26} + 7H_2 \rightarrow Pt_5H_{20}(H_2) + Pt_3H_{12}(H_2)_3$	−1.857	
$Pt_9H_{30}(H_2)_2 + 4H_2 \rightarrow Pt_5H_{20}(H_2) + Pt_4H_{16}(H_2)_2$	−3.696	0.98/2.07
$Pt_{10}H_{28}(H_2)_2 + 6H_2 \rightarrow 2Pt_5H_{20}(H_2)$	−4.479	0.93/2.03
$Pt_{10}H_{28}(H_2)_2 + 10H_2 \rightarrow 2Pt_4H_{16}(H_2)_2 + Pt_2H_8(H_2)_2$	−3.236	
$Pt_{11}H_{32}(H_2) + 9H_2 \rightarrow 2Pt_5H_{20}(H_2) + PtH_4(H_2)_2$	−4.299	0.92/2.02
$Pt_{11}H_{32}(H_2) + 12H_2 \rightarrow 2Pt_4H_{16}(H_2)_2 + Pt_3H_{12}(H_2)_3$	−4.089	
$Pt_{11}H_{32}(H_2) + 10H_2 \rightarrow Pt_5H_{20}(H_2) + Pt_4H_{16}(H_2)_2 + Pt_2H_8(H_2)_2$	−3.675	
$Pt_{12}H_{36} + 12H_2 \rightarrow 3Pt_4H_{16}(H_2)_2$	−5.730	0.89/2.00
$Pt_{13}H_{34} + 14H_2 \rightarrow Pt_5H_{20}(H_2) + 2Pt_4H_{16}(H_2)_2$	−3.403	0.92/2.08
$Pt_{13}H_{34} + 17H_2 \rightarrow 2Pt_5H_{20}(H_2) + 3PtH_4(H_2)_2$	−5.420	

[a] *a* is the total energy of adsorption per platinum atom. *b* is the cohesive energy of the saturated compound per platinum atom.

(Pt_9, Pt_{10}, Pt_{13}), the hydrogenation of metallic structures of non-optimal stability could give hydrogenated compounds of greater stability than the isomers formed from the most stable naked isomers. Thus, reorganizations of the cluster can occur under the influence of the hydrogen adsorption.

Let us now inquire about the possible fragmentation, in the presence of dihydrogen, of the large hydrogenated clusters into small units fully hydrogenated. In Table V are represented the energies of such reactions. The values for Pt_3–Pt_5 are endothermic while they are exothermic for Pt_6 and above. Besides the effect on the relative values of the metal–ligand and metal–metal interactions, the number of ligands per platinum atom decreasing with increasing cluster size explains the exothermic fragmentations. However, even if the decompositions are thermodynamically feasible, they will only be observed if a kinetically accessible path exists. According to least motion, a low-energy barrier would require an approach of the added hydrogens from the inside of the cluster. This appears not to be easily accomplished.

In Table V are also reported two indices *a* and *b* which represent the mean cohesion energy of the saturated cluster per platinum atom relatively to the naked aggregate (*a*) or to isolated atoms (*b*). Both are maximum for Pt_4. The exceptional adsorption energy of the first hydrogenation step on Pt_4 exists again in the stability of the saturated compound. Although an isolated $Pt_5H_{20}(H_2)$ cluster does not fragment, it rearranges when it is interacting with other clusters to give the cluster $Pt_4H_{16}(H_2)_2$ as shown by the reactions:

$$4Pt_5H_{20}(H_2) + 6H_2 \rightarrow 5Pt_4H_{16}(H_2)_2 \ (-0.156 \text{ eV})$$

$$Pt_5H_{20}(H_2) + Pt_3H_{12}(H_2)_3 \rightarrow 2Pt_4H_{16}(H_2)_2 \ (-1.109 \text{ eV})$$

The results on Table V show that, in presence of an excess of hydrogen, the optimal size of the platinum clusters is four. This small number contrasts with the fact that the naked clusters tend to aggregate to form a metal bulk. So, thermodynamically, in the presence of an excess of hydrogen, the large clusters would tend to fragment into small saturated pieces. This result could be related to the good stability of the very small platinum clusters on zeolites with hydrogen.[6]

VI. Conclusion and Comparison with Experiment

In zeolite, Fraissard et al. observed by xenon NMR that dihydrogen is adsorbed by small platinum clusters in a stepwise fashion.[6] From the present study, it is concluded that the stepwise procedure is specific of the small Pt_2–Pt_7 clusters since the energy of the first hydrogenation step is larger by more than 1.0 eV than the energy of the second step. For larger clusters, this energy difference is smaller and can even favor the second step (cooperative effect). This prevents the stepwise hydrogenation of these clusters. These results suggest that the cluster size used in the above-mentioned experiments is really around 4–8. If we consider that the first hydrogenation step of the Pt_3 and Pt_4 clusters has a reaction energy larger by 0.4–0.5 eV than that of the other small clusters, a first hydrogenation would take place on all the Pt_3 and Pt_4 clusters before any cluster of different size is hydrogenated and before they adsorbed themselves a second dihydrogen molecule. For the whole series of the studied clusters and on the surface of a *fcc* platinum, the first hydrogenation step is an oxidative addition which places the resulting hydride ligands in bridging positions. The structures of the hydrogenated clusters resulting from the successive steps up to the saturation can be considered as the progressive buildup of a network of complexes (mostly d^8 square planar or d^6 octahedral) sharing common ligands. The result is that the catalytic selectivity and activity of the small clusters could strongly depend on their degree of hydrogenation with either oxidative or reductive dominant properties with regard to the incoming organic substrats.

Additional Materials. Cartesian coordinates of all the intermediate structures may be obtained from the authors

Acknowledgment. This work was initiated by discussions with Professor J. Fraissard and here the authors want to thank him. They also are grateful to Professor L. Salem for fruitful comments. Financial support has been provided by the CNRS (ATP-MAT7 No. 902581).

Registry No. H_2, 1333-74-0; Pt, 7440-06-4.